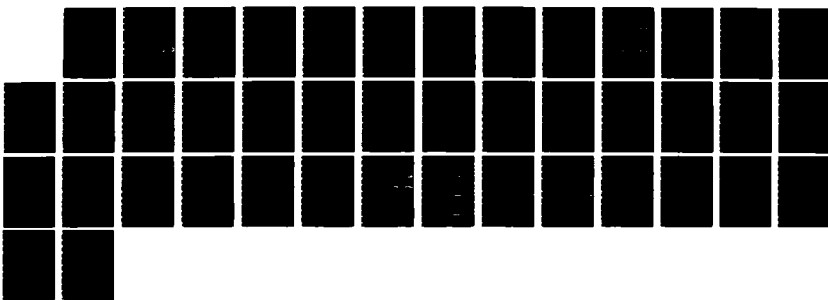
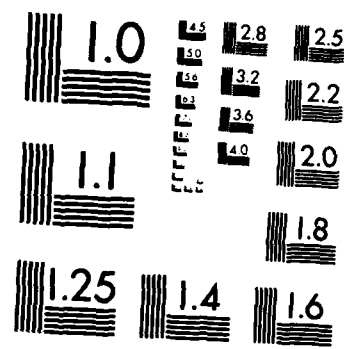


AD-A172 299 PH-SENSITIVE WO(3)-BASED MICROELECTROCHEMICAL  
TRANSISTORS(U) MASSACHUSETTS INST OF TECH CAMBRIDGE  
DEPT OF CHEMISTRY M J NATAN ET AL 22 SEP 86 TR-11  
UNCLASSIFIED N08014-84-K-0291 F/G 9/1 NL

1/1





MICROCOPY RESOLUTION TEST CHART  
NATIONAL BUREAU OF STANDARDS-1963-A

AD-A172 299

DTIC FILE COPY

SECURITY CLASSIFICATION OF THIS PAGE (When Data Entered)

(2)

| REPORT DOCUMENTATION PAGE   |                       | READ INSTRUCTIONS BEFORE COMPLETING FORM  |
|---|-----------------------|---|
| 1. REPORT NUMBER<br>ONR TR 11   | 2. GOVT ACCESSION NO. | 3. RECIPIENT'S CATALOG NUMBER   |
| 4. TITLE (and Subtitle)<br>pH-Sensitive WO <sub>3</sub> -Based Microelectrochemical Transistors   |                       | 5. TYPE OF REPORT & PERIOD COVERED<br>Interim Technical Report                    |
| 7. AUTHOR(s)<br>Michael J. Natan, Thomas E. Mallouk, Mark S. Wrighton   |                       | 6. PERFORMING ORG. REPORT NUMBER  |
| 9. PERFORMING ORGANIZATION NAME AND ADDRESS<br>Department of Chemistry<br>Massachusetts Institute of Technology<br>Cambridge, MA 02139  |                       | 10. PROGRAM ELEMENT, PROJECT, TASK AREA & WORK UNIT NUMBERS<br>Work Unit #202-261 |
| 11. CONTROLLING OFFICE NAME AND ADDRESS<br>Office of Naval Research<br>Department of the Navy<br>Arlington, VA 22217  |                       | 12. REPORT DATE<br>September 22, 1986   |
| 14. MONITORING AGENCY NAME & ADDRESS (if different from Controlling Office)   |                       | 13. NUMBER OF PAGES<br>38   |
|   |                       | 15. SECURITY CLASS. (of this report)<br>Unclassified                              |
|   |                       | 15a. DECLASSIFICATION/DOWNGRADING SCHEDULE  |
| 16. DISTRIBUTION STATEMENT (of this Report)<br><br>Approved for Public release; reproduction is permitted for any purpose of the United States Government; distribution unlimited.  |                       |   |
| 17. DISTRIBUTION STATEMENT (of the abstract entered in Block 20, if different from Report)<br><br>Distribution of this document is unlimited  |                       |   |
| 18. SUPPLEMENTARY NOTES<br><br>Prepared for publication in <u>Journal of Physical Chemistry</u>   |                       |   |
| 19. KEY WORDS (Continue on reverse side if necessary and identify by block number)<br><br>molecular electronics, microelectrochemistry, microelectrodes, surface modification, molecule based transistors, polyaniline, poly-3-methylthiophene Chemical sensors, WO <sub>3</sub> , pH-sensors |                       |   |
| 20. ABSTRACT (Continue on reverse side if necessary and identify by block number)<br><br>Attached   |                       |   |

## ABSTRACT

Electrochemical properties of an array of closely spaced ( $1.2 \mu\text{m}$ ) Au or Pt microelectrodes ( $\sim 2 \mu\text{m}$  wide  $\times \sim 50 \mu\text{m}$  long  $\times 0.1 \mu\text{m}$  high) coated by a  $0.15 \mu\text{m}$  thick layer of polycrystalline  $\text{WO}_3$  are reported. The  $\text{WO}_3$  is deposited on the electrodes by rf sputtering of a  $\text{WO}_3$  target. The cyclic voltammetry of these microelectrodes indicates that  $\text{WO}_3$  connects individual microelectrodes, since the voltammogram of a pair of microelectrodes driven together is indistinguishable from that of an individual microelectrode.  $\text{WO}_3$  becomes a good conductor upon electrochemical reduction in aqueous solutions. The change in resistance of  $\text{WO}_3$  connecting two microelectrodes as a function of electrochemical potential spans four orders of magnitude, from  $\sim 10^6$  to  $\sim 10^2$  ohms. A pair of  $\text{WO}_3$ -connected microelectrodes functions as a microelectrochemical transistor that is sensitive to pH. The cyclic voltammetry is pH-dependent and consistent with pH-dependent transistor characteristics, which indicate that the device is turned on at more positive electrochemical potentials in acidic media. In basic solutions, more negative potentials are needed to turn on  $\text{WO}_3$ -based transistors. The maximum slope of the drain current,  $I_D$ , vs. gate voltage,  $V_G$ , plot at fixed drain voltage,  $V_D$ , gives a transconductance of  $12 \text{ mS/mm}$  of gate width. Potential step and potential sweep measurements indicate that the  $\text{WO}_3$ -based transistor can be reversibly turned off and on in seconds; furthermore, the gate current,  $I_G$ , and  $I_D$  can be measured simultaneously, allowing demonstration of power gain for a sinusoidal variation of  $V_G$  at fixed  $V_D$ . Operating at a frequency of 1 Hz, the power amplification by the

WO<sub>3</sub>-based transistor is 200, at pH 1. The power amplification decreases at both higher pH and higher frequency. The properties of the WO<sub>3</sub>-based microelectrochemical transistor allow its use as a real-time pH sensor: a reproducible change in I<sub>D</sub>, at fixed V<sub>G</sub> and V<sub>D</sub>, is obtained rapidly as the pH of a stream flowed continuously past the electrode is repetitively changed from pH 3.9 to pH 7.2.



|  |                         |
|--|-------------------------|
| Accession For                                  |                         |
| NTIS GRA&I <input checked="" type="checkbox"/> |                         |
| DTIC TAB <input type="checkbox"/>              |                         |
| Unpublished <input type="checkbox"/>           |                         |
| Justification                                  |                         |
| By _____                                       |                         |
| Distribution/                                  |                         |
| Availability Codes                             |                         |
| Dist   | Avail and/or<br>Special |
| A-1  |                         |

pH-Sensitive WO<sub>3</sub>-Based Microelectrochemical Transistors

Michael J. Natan, Thomas E. Mallouk, and Mark S. Wrighton\*

Department of Chemistry

Massachusetts Institute of Technology

Cambridge, Massachusetts 02139

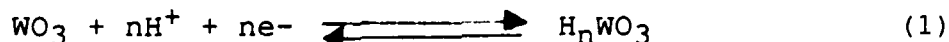
\*Address correspondence to this author.

## ABSTRACT

Electrochemical properties of an array of closely spaced ( $1.2 \mu\text{m}$ ) Au or Pt microelectrodes ( $\sim 2 \mu\text{m}$  wide  $\times \sim 50 \mu\text{m}$  long  $\times 0.1 \mu\text{m}$  high) coated by a  $0.15 \mu\text{m}$  thick layer of polycrystalline  $\text{WO}_3$  are reported. The  $\text{WO}_3$  is deposited on the electrodes by rf sputtering of a  $\text{WO}_3$  target. The cyclic voltammetry of these microelectrodes indicates that  $\text{WO}_3$  connects individual microelectrodes, since the voltammogram of a pair of microelectrodes driven together is indistinguishable from that of an individual microelectrode.  $\text{WO}_3$  becomes a good conductor upon electrochemical reduction in aqueous solutions. The change in resistance of  $\text{WO}_3$  connecting two microelectrodes as a function of electrochemical potential spans four orders of magnitude, from  $\sim 10^6$  to  $\sim 10^2$  ohms. A pair of  $\text{WO}_3$ -connected microelectrodes functions as a microelectrochemical transistor that is sensitive to pH. The cyclic voltammetry is pH-dependent and consistent with pH-dependent transistor characteristics, which indicate that the device is turned on at more positive electrochemical potentials in acidic media. In basic solutions, more negative potentials are needed to turn on  $\text{WO}_3$ -based transistors. The maximum slope of the drain current,  $I_D$ , vs. gate voltage,  $V_G$ , plot at fixed drain voltage,  $V_D$ , gives a transconductance of  $12 \text{ mS/mm}$  of gate width. Potential step and potential sweep measurements indicate that the  $\text{WO}_3$ -based transistor can be reversibly turned off and on in seconds; furthermore, the gate current,  $I_G$ , and  $I_D$  can be measured simultaneously, allowing demonstration of power gain for a sinusoidal variation of  $V_G$  at fixed  $V_D$ . Operating at a frequency of  $1 \text{ Hz}$ , the power amplification by the

WO<sub>3</sub>-based transistor is 200, at pH 1. The power amplification decreases at both higher pH and higher frequency. The properties of the WO<sub>3</sub>-based microelectrochemical transistor allow its use as a real-time pH sensor: a reproducible change in I<sub>D</sub>, at fixed V<sub>G</sub> and V<sub>D</sub>, is obtained rapidly as the pH of a stream flowed continuously past the electrode is repetitively changed from pH 3.9 to pH 7.2.

In this article we report the properties of  $\text{WO}_3$ -based microelectrochemical transistors prepared by derivatization of microelectrode arrays with polycrystalline  $\text{WO}_3$ , which undergoes the reversible, proton-dependent redox reaction shown in equation (1).<sup>1</sup>



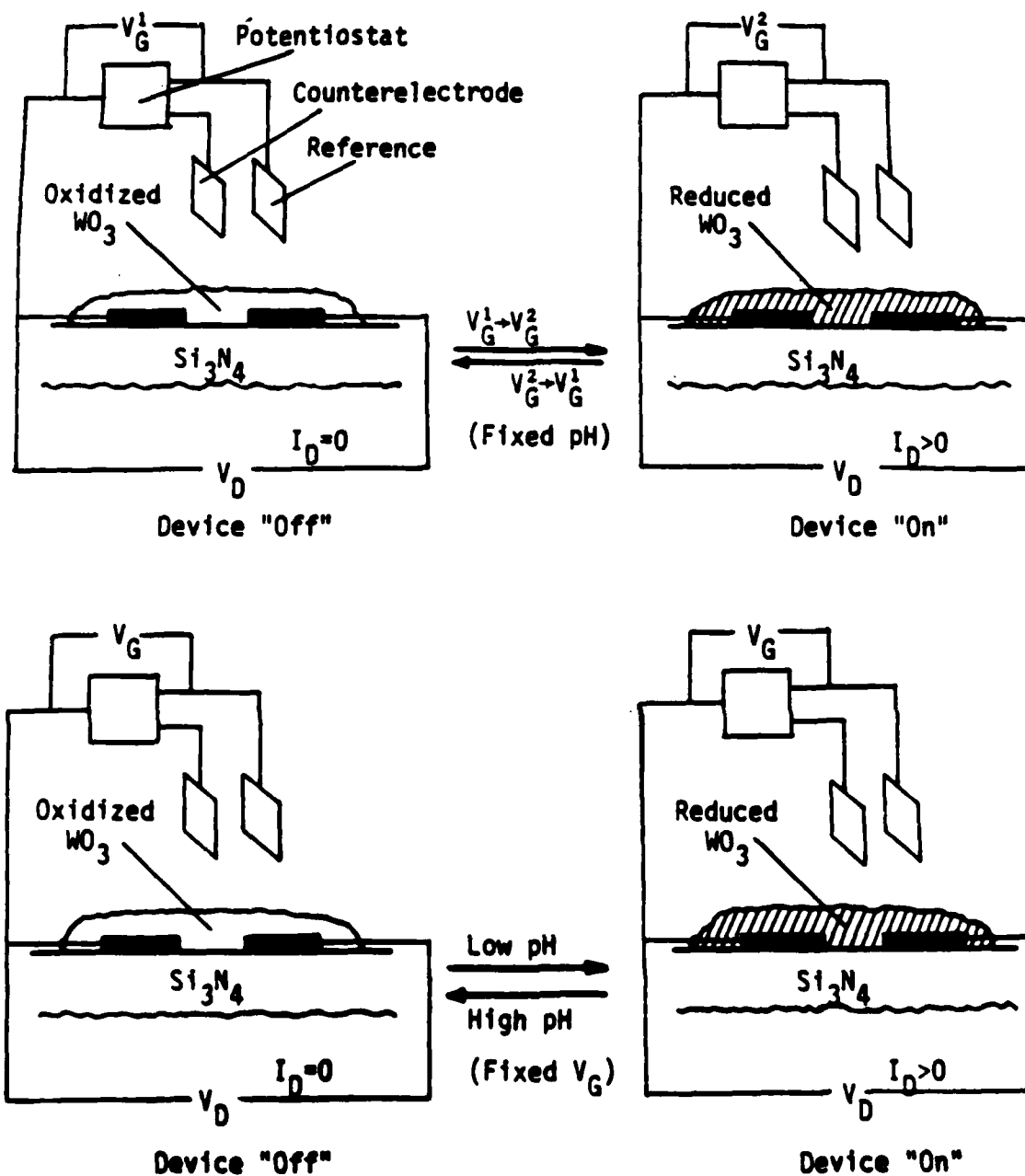
The microelectrode arrays were coated by rf plasma deposition from a sintered polycrystalline target of  $\text{WO}_3$ .  $\text{WO}_3$  has received considerable attention in recent years as an electrochromic material, because it becomes colored upon reduction.<sup>2</sup> In addition, reports on anodically grown,<sup>3</sup> polycrystalline,<sup>4</sup> colloidal,<sup>5</sup> and dispersions of<sup>6</sup> n-type semiconducting  $\text{WO}_3$  have appeared. Further interest in the material stems from the fact that the reduced, cation-intercalated species,  $\text{M}_n\text{WO}_3$  ( $\text{M} = \text{H}^+$ ,  $\text{Na}^+$ , and  $\text{Li}^+$ ), are conducting.<sup>7</sup> It is the change in conductivity of  $\text{WO}_3$  and the pH dependence of the electrochemical potential where the conductivity occurs that is crucial in demonstrating a pH-dependent microelectrochemical transistor.

Closely spaced ( $1.2 \mu\text{m}$ ) Au or Pt microelectrodes ( $\sim 2 \mu\text{m}$  wide  $\times$   $\sim 50 \mu\text{m}$  wide  $\times$   $\sim 0.1 \mu\text{m}$  high) have proven useful to the study of electroactive, conducting organic polymers that can be derivatized onto Pt or Au.<sup>8-10</sup> When the conductivity of the derivatized material can be modulated by control of the electrochemical potential of the redox active polymer, as in the cases of polypyrrole,<sup>8</sup> poly(N-methyl pyrrole),<sup>8b</sup> polyaniline,<sup>9</sup> or poly(3-methylthiophene),<sup>10</sup> the polymer-

connected microelectrodes behave as microelectrochemical transistors, in analogy to solid-state transistors.

A microelectrochemical transistor based on potential-dependent conductivity of a redox material is illustrated in Scheme I. When two closely spaced microelectrodes are connected by a redox active material such as  $\text{WO}_3$ , the current which flows between the two microelectrodes (when there is a potential difference between them) can be modulated by a change in the redox state of the redox active material. The redox state is established by the gate potential,  $V_G$ . The charge needed to electrochemically switch the material between the insulating and conducting states is associated with the gate current,  $I_G$ . The potential difference between the two microelectrodes is called the drain voltage,  $V_D$ , and the current flowing in the drain circuit is  $I_D$ . When  $V_G$  is set to  $V_G^1$ , the material is insulating,  $I_D = 0$ , and the device is off, but when  $V_G$  is moved to  $V_G^2$ , the material becomes conducting, and the device is on,  $I_D > 0$ , for a fixed value of  $V_D$ . Polypyrrole,<sup>8</sup> polyaniline,<sup>9</sup> and poly(3-methylthiophene)<sup>10</sup> are similar in that they are conducting when oxidized, and transistors based on these materials turn on at positive values of  $V_G$ .  $\text{WO}_3$ , in contrast, is insulating when oxidized, and conducting when reduced (Scheme I).  $\text{WO}_3$ -based transistors, then, are the first microelectrochemical devices which can be turned on at negative values of  $V_G$  relative to the saturated calomel reference electrode. The point is that turn on potentials are associated with reduction of the active material rather than with oxidation.

Another fundamental difference between  $\text{WO}_3$ -based devices and the previously characterized microelectrochemical transistors is that the



Scheme I. A  $\text{WO}_3$ -based transistor that turns on ( $I_D > 0$ ) when  $V_G$  is moved from  $V_G^1$  where  $\text{WO}_3$  is oxidized and insulating to  $V_G^2$  where  $\text{WO}_3$  is reduced and conducting. The  $\text{WO}_3$ -based device can also be turned on and off by varying the pH at fixed  $V_G$ .

reduction to the conducting state involves intercalation of cationic species (in aqueous solutions, protons) into the solid. This has two consequences, the first being that response time, the amount of time necessary to switch from the conducting state to the insulating state and back, is limited by the diffusion coefficient of protons within the oxide, which can be small.<sup>11</sup> The second consequence of the presence of H<sup>+</sup> in equation (1) is that the reduction of WO<sub>3</sub> is pH-dependent. Thus, the V<sub>G</sub> required to turn on the device, V<sub>G</sub><sup>2</sup>, varies with pH. At a given V<sub>G</sub> and V<sub>D</sub>, a change in pH causes a change in the ratio of oxidized to reduced WO<sub>3</sub>, causing a change in I<sub>D</sub>, as illustrated in Scheme I. Thus, a WO<sub>3</sub>-based microelectrochemical transistor functions as a pH sensor over a wide range of pH. Several other microelectrochemical transistors based on closely spaced microelectrodes connected by pH-sensitive electroactive materials have been developed by the Wrighton group,<sup>12</sup> including those based on platinized poly(3-methylthiophene),<sup>10b,13</sup> a viologen/quinone polymer,<sup>14</sup> and ferrocyanide-loaded, protonated poly(4-vinylpyridine).<sup>15</sup> The system based on WO<sub>3</sub>-connected microelectrodes is the simplest, and operates over the widest range of pH's. Aside from WO<sub>3</sub>, there are many other transition metal oxides that could function in microelectrochemical devices. Nb<sub>2</sub>O<sub>5</sub>,<sup>2a,16</sup> MoO<sub>3</sub>,<sup>2a,17</sup> IrO<sub>2</sub>,<sup>18</sup> and RhO<sub>2</sub><sup>18a,19</sup> are examples of rugged oxides that can be switched electrochemically between conducting and insulating states by intercalation reactions similar to equation (1). A study of pH-sensitive Ni(OH)<sub>2</sub>-based microelectrochemical transistors has recently been completed.<sup>20,21</sup>

### EXPERIMENTAL SECTION

Preparation, Masking, Cleaning, and Encapsulation of Eight Wire Microelectrode Arrays. The microelectrode arrays used in these experiments were of a design described previously.<sup>8-10</sup> The chips were masked prior to WO<sub>3</sub> deposition to ensure deposition on the array only either by manually applied aluminum foil masks or by photolithographically prepared Si<sub>3</sub>N<sub>4</sub> masks 0.1 μm thick. Immediately prior to deposition of WO<sub>3</sub>, the masked devices were cleaned by an O<sub>2</sub> plasma using a Harrick Plasma Cleaner. The chamber containing the samples was evacuated and backfilled with O<sub>2</sub> to a pressure of 160 microns. The plasma was formed and the samples were treated for 10 min. After deposition of WO<sub>3</sub>, electrical contact to individual wires was made and the devices were encapsulated in the usual fashion.<sup>8c</sup>

Deposition of WO<sub>3</sub>. The deposition of WO<sub>3</sub> was accomplished using a modification of a literature procedure.<sup>22</sup> Polycrystalline WO<sub>3</sub> was sputtered downhill from a sintered polycrystalline WO<sub>3</sub> target onto half-masked macroscopic Au, Pt, and SnO<sub>2</sub> electrodes, and onto masked microelectrodes using an R. D. Matthis SP 310 RF diode sputtering system. The power was provided by an RF Plasma Products power supply. The diameter of the cathode was 3.5 inches. The samples were initially presputtered for 15 minutes for further cleaning. Deposition then took place onto the heated (676K) samples for 8 to 12 minutes, depending on the thickness of WO<sub>3</sub> desired. The sputtering gas was a 10% O<sub>2</sub>/Ar mixture for both the presputtering and the actual deposition. These conditions allowed preparation of many samples

simultaneously, all having a coating of  $\text{WO}_3$  of thickness 0.1-0.2  $\mu\text{m}$  (depending on the sputtering time).

Measurement of Sample Thickness. Step profiles on  $\text{WO}_3$  microelectrodes were measured using either a Tencor Instruments Alpha-Step 100 or a Sloan Dektak surface profiling system. Both macroscopic electrodes and microelectrodes gave the same thickness ( $\pm 20\%$ ) for a given deposition. Step heights as small as 0.03  $\mu\text{m}$  were measurable under favorable conditions.

Chemicals and Solutions. The  $\text{H}_2\text{O}$  used for all experiments was Omnisolv HPLC grade. The electrolytes were all commercially available and used as obtained. Unbuffered solutions, when used, were rigorously deoxygenated and kept under  $\text{N}_2$  in order to maintain a constant pH value.

Equipment. Electrochemical experiments were performed using Pine Instruments RDE-4 bipotentiostats and Kipp and Zonen X-Y-Y' or X-Y recorders for microelectrodes and a PAR 173/175 potentiostat/programmer in conjunction with a Houston 2000 X-Y recorder for macroscopic electrodes. The Kipp and Zonen recorders or Tektronix storage oscilloscopes with camera attachments were used for time based experiments. A sinusoidal waveform was obtained using the internal oscillator output of a PAR 5204 lock-in amplifier. UV-visible spectra were recorded using either a Hewlett-Packard Model 8451-A diode array spectrophotometer or a Cary 17 spectrophotometer. Optical micrographs of microelectrodes were obtained with a Polaroid camera mounted on a Bausch and Lomb Model optical microscope. Reproducible chemical signals were delivered to microelectrodes using the two pumps of a Hewlett-Packard Model 1084B high pressure liquid chromatograph.

## RESULTS AND DISCUSSION.

Characterization of RF Sputtered Films of WO<sub>3</sub> on Macroscopic Electrodes. The electrochemistry of thin films of polycrystalline WO<sub>3</sub> on optically transparent SnO<sub>2</sub> electrodes was examined at pH 4.5. As expected for the WO<sub>3</sub> electrochromic material,<sup>2</sup> intense coloration in the visible region accompanies electrochemical reduction, as shown in Figure 1. The significant changes in the absorbance at 700 nm occur from -0.3 to -0.8 V vs. SCE, where reduction is observed by cyclic voltammetry. The inset to Figure 1 shows the actual spectra after subtraction of the optical spectrum of the completely oxidized electrode. No significant spectral changes occur beyond -1.0 V vs. SCE for WO<sub>3</sub> at pH 4.5. The electrochemical potential of the cyclic voltammetric wave (and of coloration) moves with pH: at pH 0, less reducing potentials are needed to reduce the WO<sub>3</sub>, while basic solutions necessitate more reducing potentials to reduce the WO<sub>3</sub>.

Potential step measurements confirm that charge can be reversibly added to and withdrawn from WO<sub>3</sub>. At pH 4.5, integrated currents from potential steps from +0.6 V to more reducing potentials indicate that at potentials negative of -0.4 V vs. SCE, "metallic" behavior is obtained, as judged by linearity of charge vs. potential plots on macroscopic SnO<sub>2</sub> and Au electrodes.<sup>10</sup> The data indicate that WO<sub>3</sub> has a capacity of approximately 100 F/cm<sup>3</sup>, somewhat smaller than that for poly(3-methylthiophene).<sup>10</sup>

Cyclic Voltammetry of WO<sub>3</sub>-Coated Microelectrodes. The cyclic voltammetry of arrays of microelectrodes coated with a 0.15 μm layer of WO<sub>3</sub> is depicted in Figure 2. The voltammograms we obtain on SnO<sub>2</sub>,

Au, and Pt macroelectrodes have the same shape as those in Figure 2 for the microelectrodes. In all cases the cyclic voltammetry is invariant with time in acidic, neutral, and basic solutions. The shape of cyclic voltammograms of  $\text{WO}_3$  have been modelled by Reichman *et al.*<sup>11</sup> Their results indicate that the shape depends, among other factors, on  $k_f$ , the charge transfer rate constant, and on the hydrogen atom diffusion coefficient within the film,  $D_H$ .<sup>11</sup> Our data is consistent with a material having a small  $D_H$  ( $\sim 1 \times 10^{-9} \text{ cm}^2/\text{sec}$ ) and  $k_f$  ( $\sim 10^{-2} \text{ sec}^{-1} (\text{mole}/\text{cm}^3)^{-2}$ ). The consequences of small values for  $D_H$  and  $k_f$  are a slow response time (manifested as a delay in oxidation of reduced  $\text{WO}_3$  upon scan reversal). Anodically grown  $\text{WO}_3$ , which has rapid response time, has larger values for both  $D_H$  ( $\sim 5 \times 10^{-8} \text{ cm}^2/\text{sec}$ ) and  $k_f$  ( $\sim 7.2 \text{ sec}^{-1} (\text{mole}/\text{cm}^3)^{-2}$ ).<sup>11</sup>

Notwithstanding the irregularly shaped cyclic voltammetry, the importance of the data in Figure 2 rests in the fact that it shows that adjacent microelectrodes of the array are electrically connected with  $\text{WO}_3$  and that charge transport within the oxide is rapid compared to the scan rate. At a given sweep rate, the cyclic voltammograms of wire A, wire B, and of wires A and B driven together are identical. The point is that all of the electroactive  $\text{WO}_3$  is addressable by each wire; if the wires were not electrically connected, or if charge transport were slow on the timescale of the voltage sweep (as can be the case with a slow oxide like  $\text{Ni(OH)}_2$ <sup>20,21</sup> or a redox polymer<sup>8</sup>), the cyclic voltammogram of the two wires driven together would equal the sum of the individual voltammograms. At sufficiently thin coatings (< 0.05  $\mu\text{m}$ ), rf sputtered or thermally grown<sup>21</sup> polycrystalline  $\text{WO}_3$  does

not connect adjacent wires and the array behaves as eight individually addressable microelectrodes.

Integration of the voltammograms in Figure 2 indicates roughly  $6 \times 10^{-8}$  C is associated with the electrochemical process upon scanning from +0.2 to -0.4 V vs. SCE. Assuming that the density of  $\text{WO}_3$  on the microelectrodes is that of the pure material, and that the surface area of  $\text{WO}_3$  on the microelectrode array is  $7 \times 10^{-9} \text{ m}^2$  (five times the area bounded by the wires themselves), and further assuming a one electron reduction per  $\text{WO}_3$  unit, one can calculate that, as a lower limit, approximately 2.5% of the total quantity of  $\text{WO}_3$  in electrical contact with the wires is reversibly reduced and reoxidized in a single scan from +0.2 to -0.4 V vs. SCE.

Resistance of  $\text{WO}_3$  as a Function of Electrochemical Potential. The resistance of  $\text{WO}_3$  connecting two (or more) microelectrodes can be measured by bringing both electrodes to a given  $V_G$ , and then scanning the potential of one microelectrode a small voltage ( $\sim \pm 25$  mV) about  $V_G$ . The drain voltage,  $V_D$ , is the potential difference between the two electrodes developed by scanning one microelectrode. The current passing between the electrodes can be related to the resistance using Ohm's law. By varying  $V_G$ , resistance versus  $V_G$  can be assessed.

Figure 3 shows representative resistance vs.  $V_G$  data for a  $\text{WO}_3$ -coated microelectrode array at pH 6.6. The top part of the figure illustrates the  $I_D$ - $V_D$  curves for  $\pm 25$  mV potential excursions (at 5 mV/sec) around the gate voltage,  $V_G$ . The drain current is equal to zero for  $V_D = 0$ , and the resistance is taken to be the reciprocal of the slope at this point. The data in Figure 3(b) indicate that the resistance changes by over three orders of magnitude from 0.0 to -0.9

V vs. SCE at pH 6.6. For particular samples, the resistance may reach limits of just over  $10^2$  and  $10^7$  ohms, but the resistance of the material never changes by more than four orders of magnitude in aqueous solution. Thus, unlike the conducting organic polymers polyaniline<sup>9</sup> and poly(3-methylthiophene),<sup>10</sup>  $\text{WO}_3$  does not exhibit very high resistance in the insulating state. The resistivity of as deposited  $\text{WO}_3$  is extremely dependent on deposition conditions, varying from  $10^3$  ohm-cm to  $10^9$  ohm-cm.<sup>2b</sup> Since polycrystalline  $\text{WO}_3$  is an n-type semiconductor, the conductivity of the material is expected to reasonably high in electrolyte-containing solutions, where the concentration of potentially doping impurities is high.

The ruggedness of the oxide, relative to conducting organic polymers,<sup>8-10</sup> is evidenced by the stability of the material in the fully reduced (conducting) state. Excursions to -1.5 V vs. SCE, 250 mV negative of the  $V_G$  of maximum conductivity (at pH 7), do not cause any irreversible damage to the oxide; in contrast, if poly(3-methylthiophene), for example, is brought to an oxidizing potential substantially more positive than where the maximum conductivity is found, irreversible chemical oxidation occurs and the polymer is degraded.<sup>10</sup>

#### pH-Dependence of the Transistor Properties of $\text{WO}_3$ -Connected

Microelectrodes. The dependence on pH of the reduction of  $\text{WO}_3$  causes the transistor properties of  $\text{WO}_3$ -connected microelectrodes to also vary with pH. We have characterized the properties of  $\text{WO}_3$ -based transistors as a function of pH. The left side of Figure 4 illustrates the cyclic voltammetry of  $\text{WO}_3$ -connected microelectrodes at acidic, neutral, and basic values of pH. As expected by equation (1),

the reduction occurs at more negative potentials at basic pH, and at more positive potentials at acidic pH. In addition, there is a slight decrease in the amount of charge injected at basic pH, as reflected by integration of the voltammograms. When the pH is lowered, the cyclic voltammogram is identical to that obtained initially in acidic solution. There may be a reversible pH-induced structural change which blocks a percentage of  $\text{WO}_3$  sites to reduction. The same phenomenon has been observed, to a greater extent, with  $\text{Ni(OH)}_2$ -coated microelectrodes.<sup>20,21</sup> The right side of Figure 4 shows, at the same three pH's, linear plots of  $I_D$  vs.  $V_D$  (at fixed  $V_G$ ) for several  $V_G$ 's, that also show a pH dependence. Thus, at  $V_G = -0.2$  V vs. SCE, the device is completely turned off at pH 12.3 (judging from the lack of drain current for any  $V_D$ ), slightly on at pH 6.6, and nearly fully turned on at pH 0. At a given pH, the slope of the  $I_D$ - $V_D$  plots increases as  $V_G$  is moved negatively, again illustrating that the resistance between  $\text{WO}_3$ -connected microelectrodes decreases as  $\text{WO}_3$  is reduced.

Another way to quantitatively assess the effect of  $V_G$  on the conductivity of a  $\text{WO}_3$  film is to measure  $I_D$  as a function of  $V_G$ , at a fixed  $V_D$ . The results of such a measurement, for three different values of pH, are plotted in Figure 5. The  $I_D$ - $V_G$  characteristic, like the resistance- $V_G$  plots of Figure 3 and the transistor curves in Figure 4, result from properties intrinsic to  $\text{WO}_3$ : the values of  $V_G$  which give significant  $I_D$ , the maximum slope of the curve (the transconductance), and the maximum value of  $I_D$  (for a given  $V_D$ ) may be expected to differ from material to material. As expected, the  $I_D$ - $V_G$  curves depend on the pH. The maximum drain current obtained for a 200

mV drain voltage is 550  $\mu$ A, which exceeds that achieved with polypyrrole,<sup>8</sup> or polyaniline,<sup>9</sup> but is less than the 1 mA found for poly(3-methylthiophene)-based devices of the same geometry.<sup>10</sup> The  $I_D$  for this particular device is approximately a factor of 5 higher than could be expected from the data in Figure 3, illustrating the sample to sample variability in resistance mentioned above. The reduced state of  $WO_3$  is several orders of magnitude more conductive than the conducting (oxidized) state of  $Ni(OH)_2$ ,<sup>20,21</sup> indicating that a large variation in  $I_D$ - $V_G$  characteristics may be found among metal oxide-based microelectrochemical devices. It is important to note that the maximum drain current of 550  $\mu$ A is achievable at pH = 7 by moving  $V_G$  to a strongly reducing potential; thus, at pH = 7 the entire  $I_D$  range of the device is accessible. Under basic conditions, an  $I_D$  of 550  $\mu$ A cannot be obtained at any  $V_G$ . The maximum slope of the  $I_D$  vs.  $V_G$  plot, transconductance, at pH 0, is around 12 mS/mm of gate width, an order of magnitude less than that obtained for poly(3-methylthiophene).<sup>10</sup> At pH 6.6, the transconductance is approximately 10 mS/mm of gate width.

The data in Figure 5 illustrate how  $WO_3$  might be used as a pH sensor, since a steady state measurement at fixed  $V_G$  and  $V_D$  gives an  $I_D$  which is solely a function of pH, presuming that other cations in solution, which are capable of intercalation into  $WO_3$ ,<sup>7</sup> do not interfere with the pH response. We have carried out several experiments to ascertain whether  $Li^+$ ,  $Na^+$ , and  $K^+$  affect the transistor behavior of  $WO_3$ -based microelectrochemical devices, and find that their effect is minimal. For example, a  $WO_3$ -based microelectrochemical transistor was placed in  $\mu = 0.05$ , pH 5 acetate

buffer with  $V_G = 0.0$  V vs. SCE and  $V_D = 150$  mV. A stable  $I_D$  of 265 nA was produced.  $\text{Li}^+$  was added in the form of  $\text{Li}_2\text{SO}_4$  to a concentration of 0.32 M. The  $I_D$  moved to 280 nA, a change of only ~6% for a four order of magnitude excess of interfering ion. Another experiment probed the effect of interfering ions on  $I_D$ - $V_D$  plots for various  $V_G$ 's (Cf. Figure 4). Saturated KCl and NaCl solutions, and 2 M LiCl (all at pH 7) gave  $I_D$ - $V_D$  plots identical to those obtained in 0.1 M  $\text{Na}_2\text{SO}_4$  (at pH 7). Also, addition of base to a pH 0.5, 2 M LiCl solution caused the  $V_G$  for turn on to move to more reducing potentials. These experiments indicate that interference of  $\text{K}^+$ ,  $\text{Na}^+$ , and  $\text{Li}^+$  is negligible in  $\text{WO}_3$ -based microelectrochemical transistors operated in aqueous solutions.

Microelectrochemical transistors are fundamentally different from solid state devices in that ionic movement is necessary to bring the material on a microelectrode to a conducting state. In the case of a solid state field effect transistor (FET), for example, source-drain current is merely a consequence of capacitative charging of the gate region, with no accompanying ionic movement.<sup>23</sup> Thus, ionic diffusion associated with faradaic processes places an upper limit on the on/off time for microelectrochemical transistors, and the response times can never be equal to those of solid state devices of the same dimensions. For the  $\text{WO}_3$  used in this study, there are further limitations imposed by small values for  $k_f$  and  $D_H$ , as shown by the cyclic voltammetry in Figures 2 and 4. Thus,  $\text{WO}_3$ -based microelectrochemical transistors exhibit response times slower than those of previously characterized microelectrochemical devices.<sup>8-10</sup>

Figure 6 shows data pertaining to the response time of a  $\text{WO}_3$ -based transistor upon stepping from a potential of +0.4 V to 0.0 V vs. SCE, at pH 5. With a pulse width of 5 seconds,  $I_D$  varies between 0 and ~8.5 nA. The magnitude of  $I_D$  indicates that this particular sample of  $\text{WO}_3$  was among the most resistive we have tested. The initial response time for both turn-on and turn-off is approximately 0.1 sec. After thirty minutes of continuous pulsing, there is deterioration in the response time, as  $I_D$  has lost a measure of rectangularity. After eight hours of continuous cycling, there is a very noticeable slowing of the response. The device neither turns fully on or off within the five second pulse width. In addition, the sluggish response is further manifested upon potential steps to more conducting states, where the completely on/completely off response time is measured in minutes, rather than seconds. It is possible that repeated potential steps on this particularly resistive sample caused structural changes which significantly affected  $k_f$  or  $D_H$ .

To the list of factors affecting response time of  $\text{WO}_3$ -based transistors may be added the thickness of the oxide on the microelectrode array. The expectation that response time would improve as the quantity of derivatized  $\text{WO}_3$  decreases is a realistic one, though at some point the connection between microelectrodes would be severed. Experiments with new microelectrode geometries will be undertaken to realize this expectation. For a given set of deposition conditions and a given thickness, a useful illustration of device response is the phase relationship of  $V_G$ ,  $I_D$ , and  $I_G$ , depicted in Figure 7 at 1 Hz, at pH 1.  $V_G$  is varied sinusoidally from +0.5 V to -0.5 V vs. SCE at a frequency of 1 Hz. In theory, at 0.5 V vs. SCE,  $I_G$

will always equal zero, as the device is fully off. Scanning negatively should result in cathodic current,  $I_G$ , associated with reduction of  $WO_3$  in the gate region. Furthermore,  $I_G$  should also equal zero at -0.5 V vs. SCE, when the device is fully on, since all the electroactive  $WO_3$  has been reduced. Scan reversal would then lead to anodic  $I_G$  associated with oxidation of the reduced  $WO_3$ . At +0.5 V vs. SCE, the  $WO_3$  is fully oxidized, and  $I_G$  is again zero. If  $I_G$  behaves ideally, then, it will be 90° out of phase with the  $V_G$ (peak).  $I_D$  should also be zero at +0.5 V vs. SCE, when the device is off, but should reach its maximum value at -0.5 V vs. SCE, when the device is expected to be fully turned on. Thus,  $I_D$  should be exactly in phase with  $V_G$ . Figure 7 shows that while  $I_D$  is in phase with  $V_G$ ,  $I_G$  is slightly more than 90° out of phase with  $V_G$ . Even at 1 Hz,  $I_G$  cannot keep up with  $V_G$ . At higher frequency,  $I_D$  maintains its phase relationship to  $V_G$  more closely than does  $I_G$ , but leakage  $I_D$  (residual  $I_D$  when the device should be completely off), barely noticeable at 1 Hz, becomes quite prominent. In addition, the magnitude of  $I_D$  declines at higher frequency, indicating that the devices are not turning on fully. Results with conducting organic polymers derivatized on microelectrodes indicate that their behavior is a much closer approximation to ideal behavior at 1 Hz, and in some cases, much higher frequencies; polyaniline-based transistors can be switched on and off at frequencies up to 1 kHz.<sup>24</sup>

The power amplification,  $A$ , observed for the data in Figure 7 can be calculated using equation (2), and is found to be 200, since

$$\underline{A} = \frac{\text{Average Power in drain circuit}}{\text{Average Power in gate circuit}} = \frac{P_{\text{drain}}}{P_{\text{gate}}} \quad (2)$$

$V_G(\text{peak}) = 1.0 \text{ V}$ ,  $V_D = 0.5 \text{ V}$ ,  $I_D(\text{peak}) = 44 \mu\text{A}$ , and  $I_G(\text{peak}) = 0.11 \mu\text{A}$ .  $I_G$  is at best proportional to the scan rate, or switching frequency, and so  $\underline{A}$  decreases monotonically at higher frequencies. By 10 Hz,  $\underline{A}$  is reduced to 2; at 100 Hz, the charging current associated with  $I_G$  exceeds  $I_D$  and there is no power amplification ( $\underline{A} < 1$ ). At these frequencies  $I_G(\text{peak})$  continues to be more than  $90^\circ$  out of phase with  $V_G(\text{peak})$ , and  $I_D(\text{peak})$  continues to be in phase with  $V_G$ , although its magnitude has declined and leakage current is significant. At pH  $> 1$ , the response time of  $\text{WO}_3$ -based transistors is slower. For example, at pH 7, a power amplification of 36 is obtained at  $3 \times 10^{-2}$  Hz, and power gain declines to 1 at less than 1 Hz.

While the power amplification and response time for  $\text{WO}_3$ -based devices are much poorer than those of solid state devices,<sup>23</sup> the important result from Figures 4,5, and 7 is that they show that  $\text{WO}_3$ -connected microelectrodes are indeed chemically based transistors that function reproducibly. All the characteristics usually associated with conventional transistors, namely changes in the slopes of  $I_D$  vs.  $V_D$  plots as  $V_G$  is varied (Figure 4), sigmoidal plots of  $I_D$  vs.  $V_G$  at fixed  $V_D$  (Figure 5), and power amplification with well-behaved and separately measurable  $I_G$  and  $I_D$  (Figure 7), have been demonstrated. Thus, the analogy between solid state transistors and microelectrochemical transistors is complete; actuation by and

amplification of electrical signals has been achieved, though not on a competitive basis with solid state devices.

The possibility of achieving far better response time with  $\text{WO}_3$ -based microelectrochemical transistors depends on two factors: improving deposition conditions and improving microelectrode geometry. Optimization of the deposition conditions with respect to response time for the  $\text{WO}_3$  used in this work has been not been attempted. For instance, it is known that addition of  $\text{H}_2\text{O}$  to the plasma produces more porous, faster responsive films of  $\text{WO}_3$ .<sup>2</sup> Undoubtedly, it is possible to derivatize microelectrode arrays with  $\text{WO}_3$  that responds more quickly to changes in  $V_G$ . As mentioned above, a decrease in the amount of electroactive material used in connecting closely spaced microelectrodes will improve the response time. A method to achieve this without changing the thickness of  $\text{WO}_3$  is to decrease the space between the wires of the microelectrode array. The technology to significantly close the  $1.2 \mu\text{m}$  spacing currently in use, thereby reducing the volume of  $\text{WO}_3$  required to contact microelectrodes, exists.<sup>25</sup> The volume of electroactive material needed in the gate region can further be reduced by coating the tops of microelectrodes with an insulating layer of  $\text{Si}_3\text{N}_4$ .<sup>24</sup> Work is in progress to prepare microelectrode arrays of the improved geometry described. Even with the many improvements possible, chemically-based microelectrochemical transistors cannot ever achieve response times associated with solid state transistors, simply because ionic movement in the gate region of chemically-based devices cannot compete with electronic movement in the gate region of solid state devices. The potential utility of  $\text{WO}_3$ -

based transistors rests in their ability to be turned on and off by a chemical signal, as in Scheme I.

Response of WO<sub>3</sub>-based Transistors to a Reproducible, Repetitive Change in pH in a Flowing Stream. The data in Figure 5 indicate that variation in  $I_D$  should be observed upon variation of pH in a solution in contact with a WO<sub>3</sub>-based transistor at fixed  $V_G$  and  $V_D$ . This fact, coupled with the durability of WO<sub>3</sub> in aqueous solutions (stable from pH 0-13; the material is soluble, however, in heated strongly basic solutions), and the lack of interference from cations, indicates that the device should make a good pH sensor. We have tested this possibility by using the two solvent reservoirs and pumps of an HPLC to create a flowing aqueous stream whose pH can be changed in order to deliver a reproducible pH change to the microelectrode. Using  $\mu = 0.1 \text{ M}$  pH 7.2 phosphate buffer in one reservoir and  $\mu = 0.1 \text{ M}$  pH 3.9 acetate buffer in the other, we can cycle the pH of the solution flowing past the WO<sub>3</sub>-coated microelectrode. The results of this experiment are shown in Figure 8, where  $V_G = -0.5 \text{ V vs. SCE}$ ,  $V_D = 150 \text{ mV}$ , and the solvent flow rate is 6.0 ml/min.  $I_D$  is monitored over time and is found to be 0.08  $\mu\text{A}$  for the pH 7.2 solution and 0.8  $\mu\text{A}$  for the pH 3.9 solution. This  $I_D$  is less than what would be expected from Figure 5, but is consistent with the resistance data in Figure 3. The changeover from one pH to the other requires approximately 45 seconds;  $I_D$  reaches the steady state value within 90 seconds of when the transistor is exposed to the new pH solution. The stream was continuously flowed past the microelectrode for 6 h, without any degradation in the response time or the steady state  $I_D$  at either pH. Thus, a WO<sub>3</sub>-based transistor can sense changes in pH and gives large,

reproducible currents in real time. The magnitude of  $I_D$  is such that much smaller changes in pH should be detectable without further amplification of  $I_D$ .

#### CONCLUSIONS

The operation of pH-sensitive microelectrochemical transistors based on  $WO_3$ -connected microelectrodes has been demonstrated. The response time of these devices is slower and power amplification is smaller than for microelectrochemical transistors based on conducting organic polymers, but the prospect of major improvements through control of deposition conditions and microelectrode geometry is possible. Unlike previously characterized microelectrochemical devices, the conducting region is accessed by negative values of  $V_G$ . This work shows that oxide-based transistors can be durable, and that, in principle, many oxides with widely varying properties can be used to fabricate microelectrochemical devices.

The effect of pH on the transistor behavior of  $WO_3$ -connected microelectrodes has been probed; agreement with predictions based on the pH dependence of the electrochemical reduction of  $WO_3$  has been found. Real-time  $I_D$  response, at fixed  $V_G$  and  $V_D$ , to pH change in a flowing stream has been shown. The full range of  $I_D$  is achievable at pH = 7 through control of  $V_G$ . The transconductance of these microelectrochemical transistors is sufficiently large to insure significant  $I_D$  in the  $V_G$  range -0.25 to -0.8 V vs. SCE at pH  $\approx$  7, where the redox potential of many biological reducing agents are found, meaning  $WO_3$ -based devices may be of value in sensing biological molecules.

Acknowledgements. We thank the Office of Naval Research and the Defense Advanced Research Projects Agency for partial support of this research. Use of the rf sputtering facility at EIC Laboratories, Norwood, Massachusetts is gratefully acknowledged.

References

1. (a) Deb, S. K. Philos. Mag., 1973, 27, 807; (b) Faughnan, B. W.; Crandall, R. S.; Lampert, M. A. Appl. Phys. Lett. 1975, 27, 275; (c) Hersh, H. N.; Kramer, W. E.; McGee, J. H. Appl. Phys. Lett., 1975, 27, 646.
2. (a) Dautremont-Smith, W. C. Displays, 1982, 3, 3; (b) Agnihotry, S. A.; Saini, K. K.; Subhas Chandra Ind. J. of Pure and Appl. Phys., 1986, 24, 19.
3. (a) Di Quarto, F.; Di Paola, A.; Piazza, S.; Sunseri, C. Sol. Energy Mat., 1985, 11, 419; (b) Di Quarto, F.; Di Paola, A.; Sunseri, C. Electrochim. Acta, 1981, 26, 1177.
4. Desilvestro, J.; Neumann-Spallart, M. J. Phys. Chem., 1985, 89, 3684.
5. Nenadovic, M. T.; Rajh, T.; Micic, O. I.; Nozik, A. J. J. Phys. Chem., 1984, 88, 5827.
6. Erbs, W.; Desilvestro, J.; Borgarello, E.; Gratzel, M. J. Phys. Chem., 1984, 88, 4001.
7. (a) Dautremont-Smith, W. C.; Green, M.; Kang, K. S. Electrochim. Acta, 1977, 22, 751; (b) Crandall, R. S.; Faughnan, B. W. Phys. Rev. Lett., 1977, 39, 232.

8. (a) White, H. S.; Kittlesen, G. P.; Wrighton, M. S. J. Am. Chem. Soc., 1984, 106, 5375; (b) Kittlesen, G. P.; White, H. S.; Wrighton, M. S. J. Am. Chem. Soc., 1984, 106, 7389; (c) Kittlesen, G. P. Ph.D. Thesis, Massachusetts Institute of Technology, Cambridge, MA, 1985.
9. Paul, E. W.; Ricco, A. J.; Wrighton, M. S. J. Phys. Chem., 1985, 89, 1441.
10. (a) Thackeray, J. W.; White, H. S.; Wrighton, M. S. J. Phys. Chem., 1985, 89, 5133; (b) Thackeray, J. W. Ph.D. Thesis, Massachusetts Institute of Technology, Cambridge, MA, 1986.
11. Reichman, B.; Bard, A. J.; Laser, D. J. Electrochem. Soc., 1980, 127, 647.
12. Wrighton, M. S.; Thackeray, J. W.; Natan, M. J.; Smith, D. K.; Lane, G. A.; Belanger, D. Phil. Trans. Royal Soc., Ser. B, submitted.
13. Thackeray, J. W.; Wrighton, M. S. J. Phys. Chem., submitted.
14. Smith, D. K.; Lane, G. A.; Wrighton, M. S. J. Am. Chem. Soc., to be submitted.
15. Belanger, Daniel; Wrighton, M. S. J. Phys. Chem., to be submitted.

16. (a) Dyer, C. K.; Leach, J. S. J. Electrochem. Soc., 1978, 125, 23;  
(b) Reichman, B.; Bard, A. J. J. Electrochem. Soc., 1980, 127, 241.
17. (a) Arnoldussen, T. C. J. Electrochem. Soc., 1976, 123, 527; (b)  
Rabelais, J. W.; Colton, R. J.; Guzman, A. M. Chem. Phys. Lett., 1974,  
29, 131; (c) Colton, R. J.; Guzman, A. M.; Rabelais, J. W. J. Appl.  
Phys., 1978, 49, 409; (d) Dickens, P. G.; Birtill, J. J. J. Electron.  
Mat., 1978, 7, 679.
18. (a) Dautremont-Smith, W. C. Displays, 1982, 3, 67; (b) Buckley, D.  
N.; Burke, L. D. J. Chem. Soc. Faraday Trans. I, 1975, 71, 1447; (c)  
Gottesfeld, S.; McIntyre, J. D. E.; Beni, G.; Shay, J. L. Appl. Phys.  
Lett., 1978, 33, 208.
19. (a) Gottesfeld, S. J. Electrochem. Soc., 1980, 127, 272; (b)  
Burke, L. D.; O'Sullivan, E. J. M. J. Electroanal. Chem., 1978, 93,  
11.
20. Natan, M. J.; Belanger, D.; Carpenter, M. K.; Wrighton, M. S.,  
manuscript in preparation.
21. Natan, M. J. Ph.D. Thesis, Massachusetts Institute of Technology,  
Cambridge, MA, 1986.
22. Miyake, K.; Kaneko, H.; Suedomi, N.; Nishimoto, S. J. Appl. Phys.,  
1983, 54, 5256.

23. Sze, S. M. "Physics of Semiconductor Devices"; Wiley: New York, 1981.
24. Lofton, E. P.; Thackeray, J. W.; Wrighton, M. S. Science, submitted.
25. (a) Mackie, S.; Beaumont, S. P. Solid State Technology, 1985, 28, 117; (b) Elliot, D. J. "Integrated Circuit Fabrication Technolgy"; McGraw-Hill: New York, 1982.

Figure Captions

Figure 1. Optical spectral changes at 700 nm accompanying the change in potential of an optically transparent  $\text{SnO}_2$  electrode coated with a film of rf plasma-deposited polycrystalline  $\text{WO}_3$  of 0.15 micron thickness. The electrolyte was a 0.1 M, pH 4.5 acetate buffer. The inset shows the visible range absorption spectra as a function of electrochemical potential.

Figure 2. Cyclic voltammetry at four sweep rates of adjacent wires of a  $\text{WO}_3$ -coated microelectrode array driven individually and together in pH 6.6 phosphate buffer.

Figure 3. (a) Current-potential curves in pH 6.6 phosphate buffer as a function of  $V_G$ . The potential of one of the microelectrodes is varied by  $\pm 25$  mV around  $V_G$ , and  $I_D$  is measured. (b) The resistance between  $\text{WO}_3$ -coated Au microelectrodes as a function of  $V_G$ , calculated from the slopes at  $V_D = 0$  of the data in the upper portion of the figure.

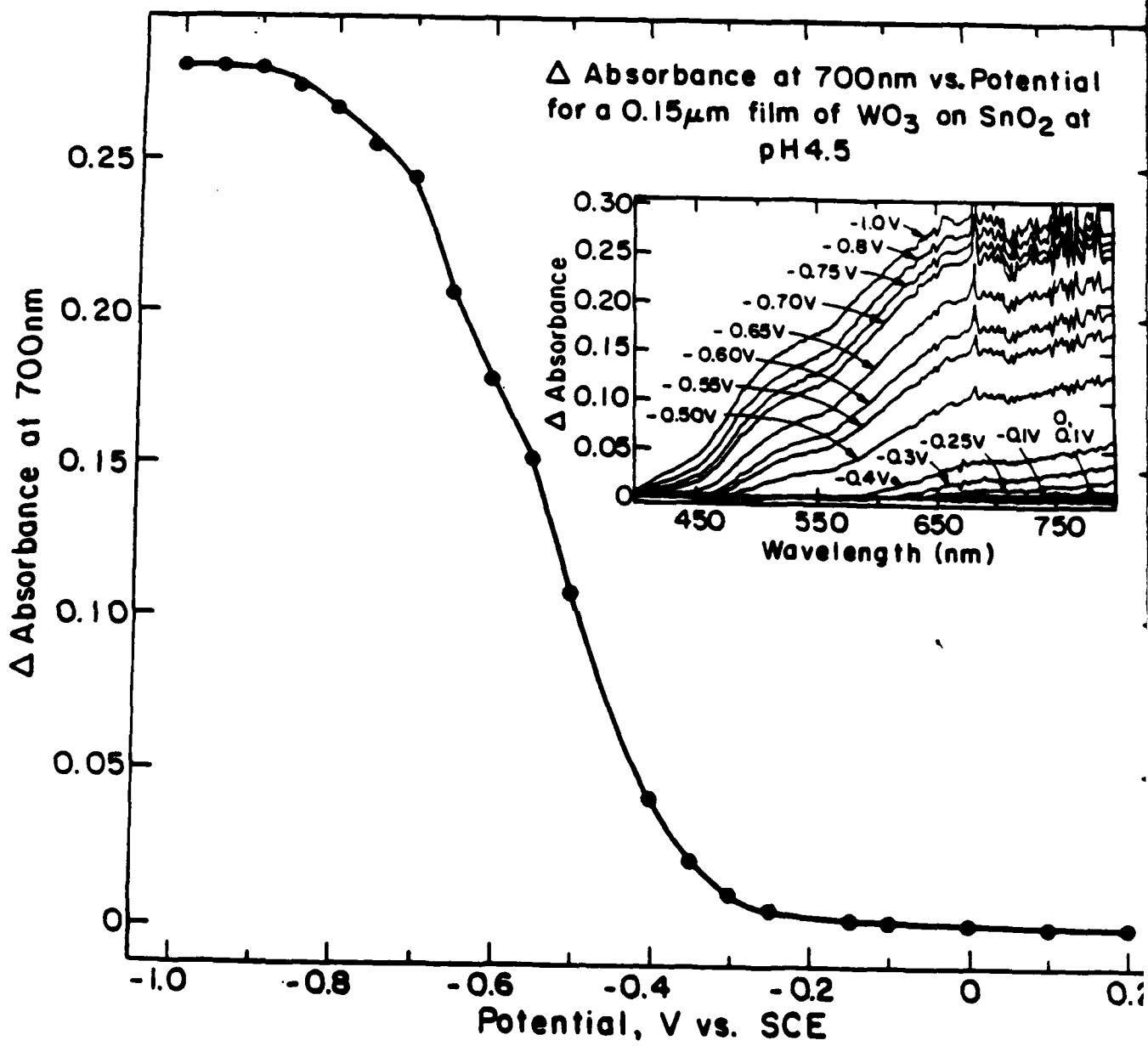
Figure 4. Cyclic voltammetry (left) and  $I_D$  vs.  $V_D$  (at fixed  $V_G$ ) transistor characteristics (right) of  $\text{WO}_3$ -connected microelectrodes at three different pH 's. The voltammograms were recorded at 200 mV/sec.  $V_D$  was varied at 10 mV/sec.

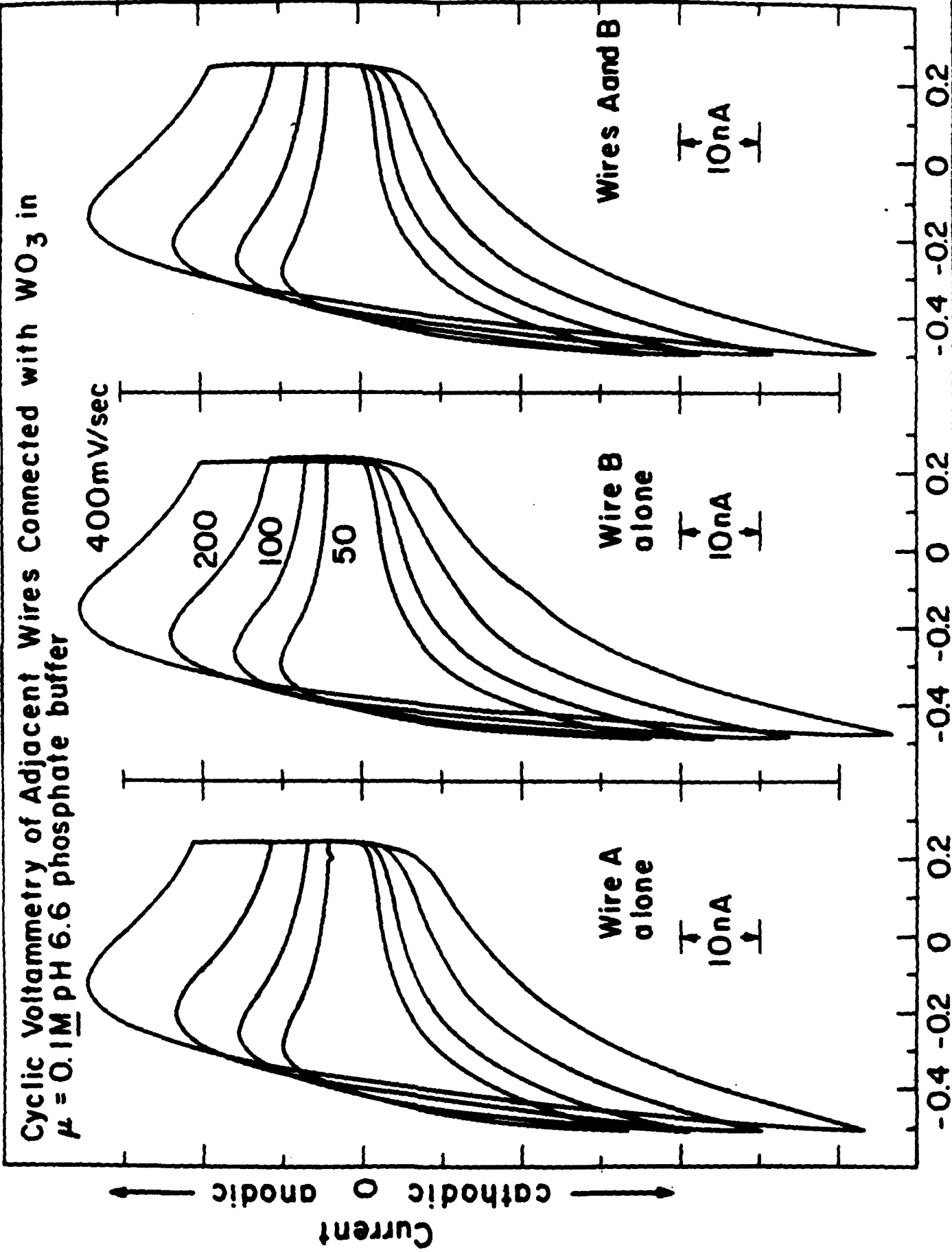
Figure 5.  $I_D$  vs.  $V_G$  at fixed (200 mV)  $V_D$  at three values of pH. These are steady state data.

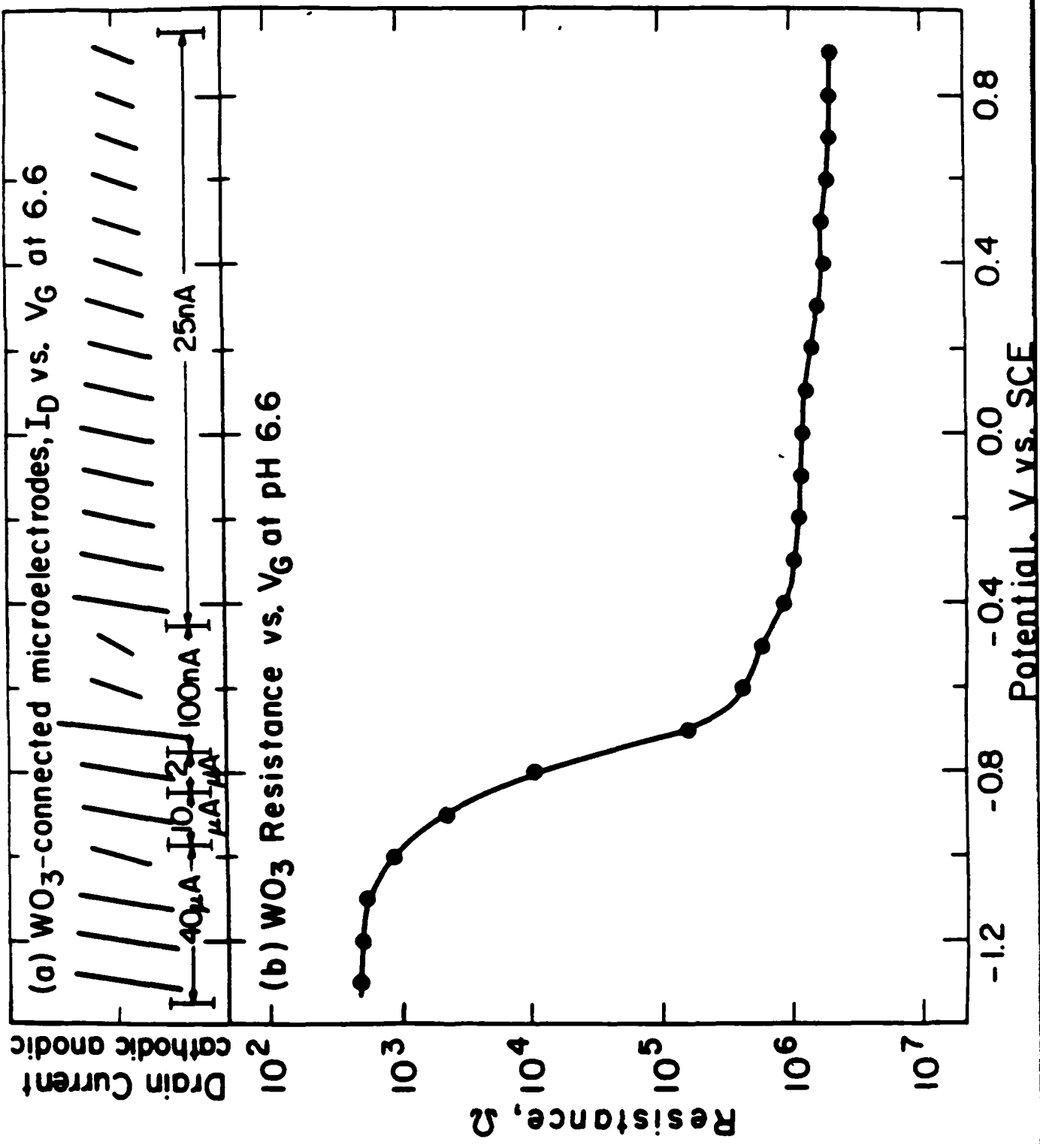
Figure 6.  $I_D$  vs. time for a  $\text{WO}_3$ -based transistor at pH 5 for a potential step from +0.4 to 0 V vs. SCE.

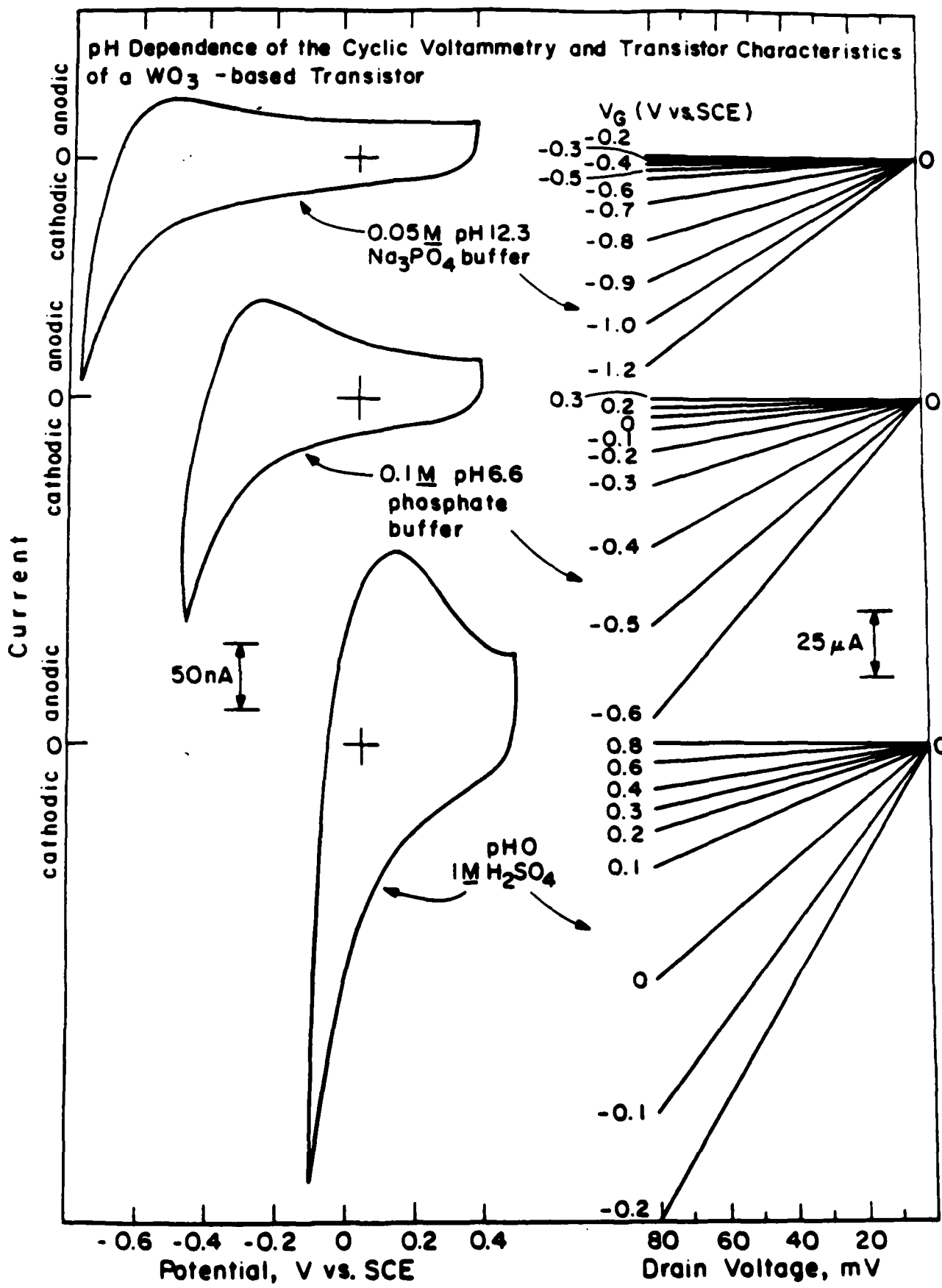
Figure 7. Phase relationship between  $V_G$ ,  $I_G$ , and  $I_D$  for a  $\text{WO}_3$ -based transistor at 1 Hz at pH 1.  $V_D = 500$  mV.  $V_G$  was varied between +0.5 and -0.5 V vs. SCE.

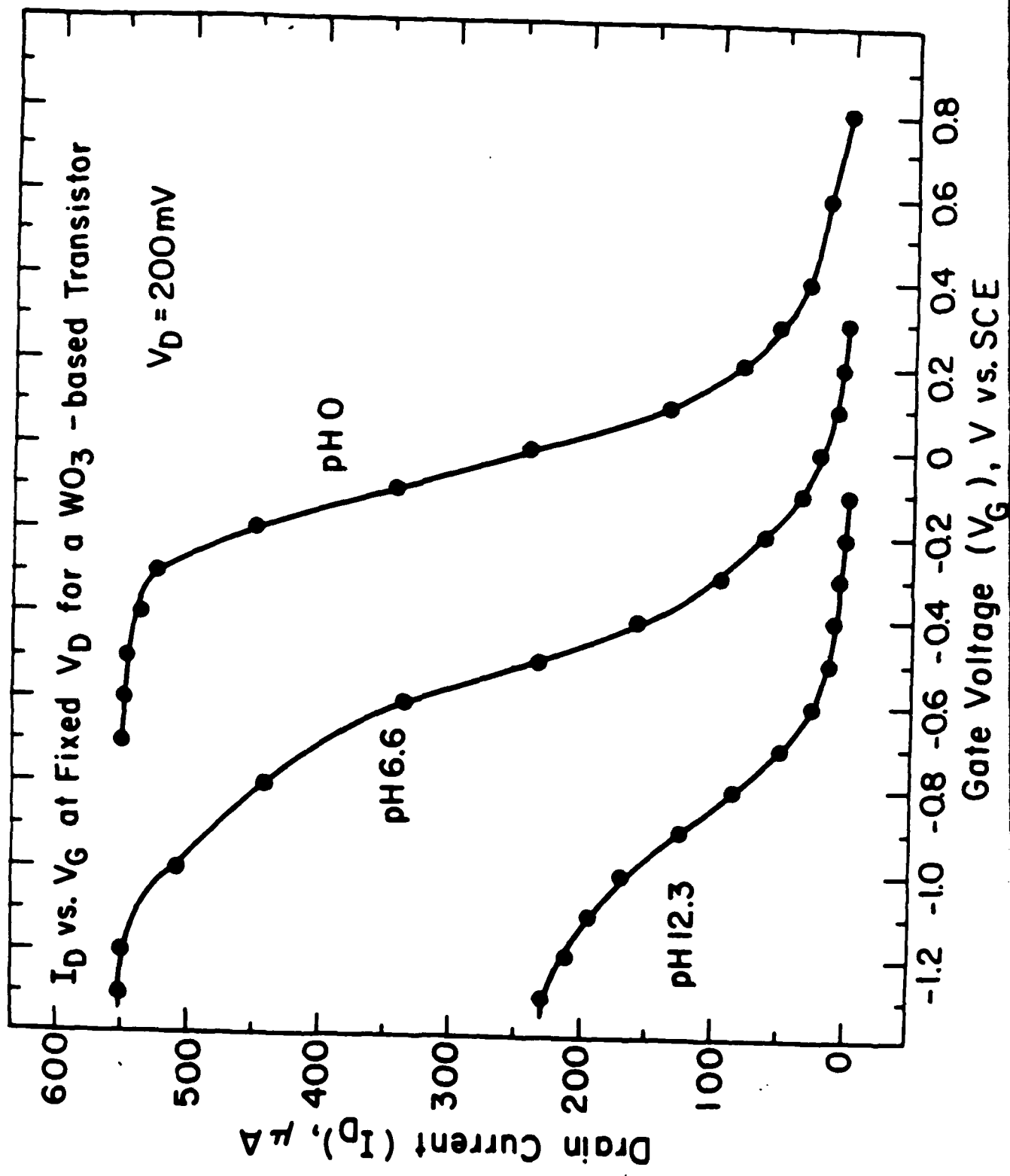
Figure 8.  $I_D$  vs. time for  $\text{WO}_3$ -based transistor upon variation of pH in a continuously flowing stream.  $V_G = -0.5$  V vs. SCE,  $V_D = 150$  mV.

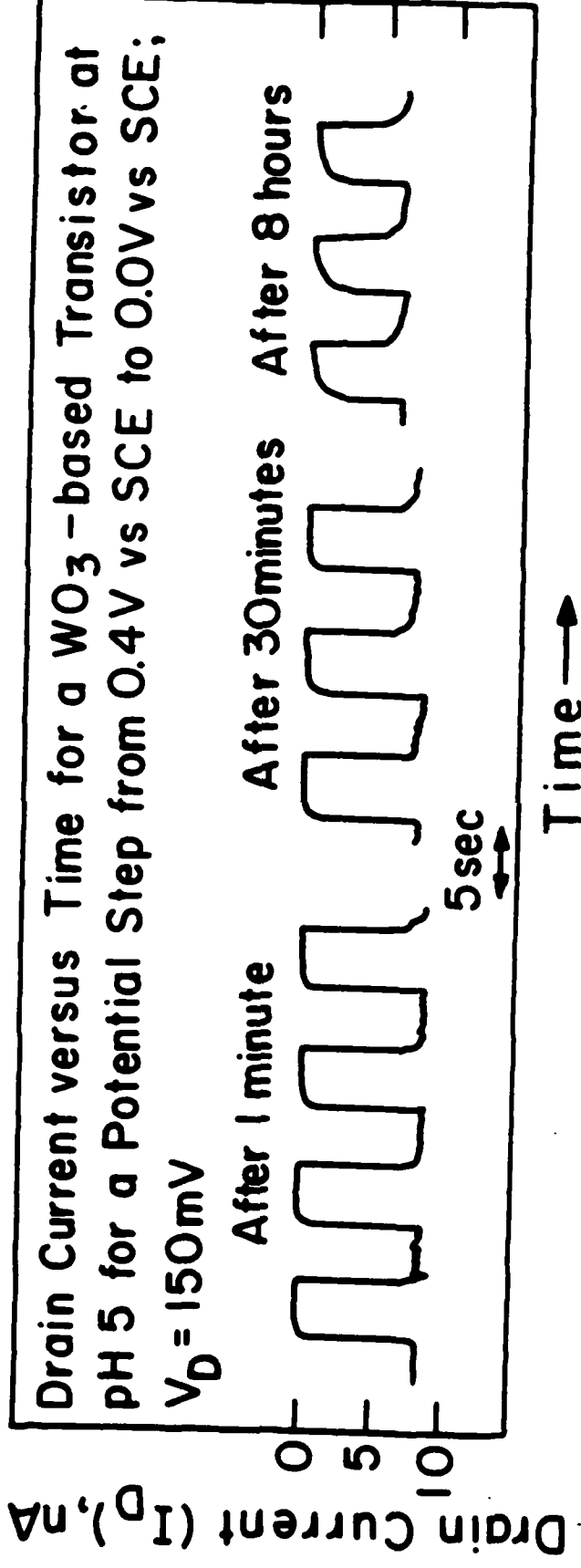




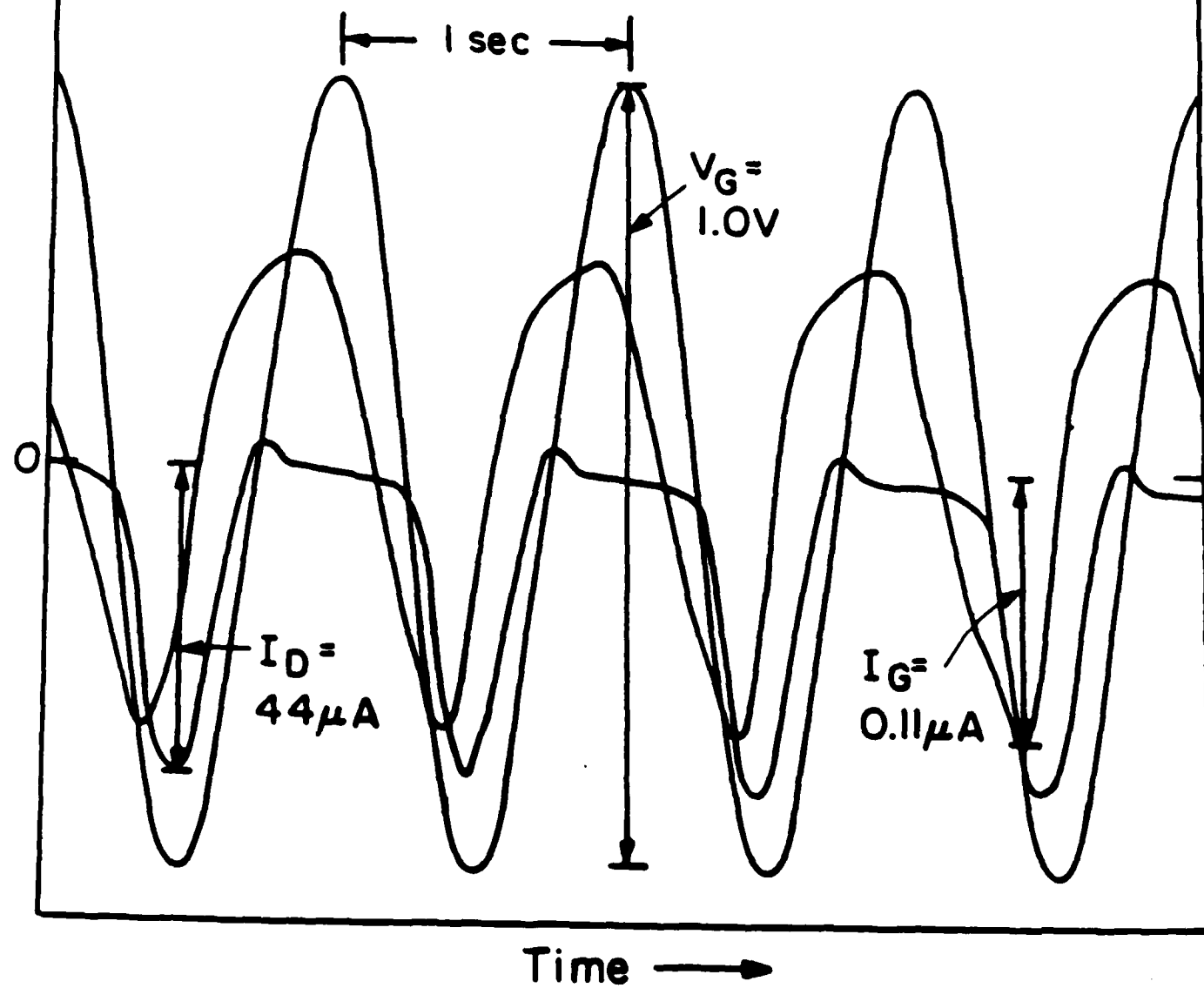








Phase Relationship Between the Gate Voltage ( $V_G$ ),  
Gate Current ( $I_G$ ), and the Drain Current ( $I_D$ ) at  
1 Hz for a  $\text{WO}_3$ -based Transistor at pH 1



**Drain Current vs. Time for a  $\text{WO}_3$  - based Transistor in Contact with a  
Continuously Flowing Two Component Stream**

$V_G = -0.5\text{V}$ ,  $V_D = 150\text{mV}$

Flow rate =  $6.0\text{ ml/min}$

$100\%\mu = 0.1\text{ M}$  phosphate pH 7.2

$100\%\mu = 0.1\text{ M}$  acetate pH 3.9

Time →

Drain Current ( $I_D$ )  $\mu\text{A}$

0      0.4      0.8

↔  
2 min

DISTRIBUTION LIST

All Reports

Molecular Biology Program, Code 441MB  
Office of Naval Research  
800 N. Quincy Street  
Arlington, VA 22217

Annual, Final and Technical Reports

Defense Technical Information Center (2 copies)  
Building 5, Cameron Station  
Alexandria, VA 22314

Annual and Final Reports Only (one copy each)

Scientific Library  
Naval Biosciences Laboratory  
Naval Supply Center  
Oakland, CA 94625

Commanding Officer

Naval Medical Research & Development Command  
National Naval Medical Center  
Bethesda, MD 20814

Director

Infectious Disease Program Center  
Naval Medical Research Institute  
National Naval Medical Center  
Bethesda, MD 20814

Commander

Chemical and Biological Sciences Division  
Army Research Office  
Research Triangle Park, NC 27709

Commander

U.S. Army Research and Development Command  
Attn: SGRD-PLA  
Fort Detrick  
Frederick, MD 21701

Commander

USAMRIID  
Fort Detrick  
Frederick, MD 21701

Commander

Air Force Office of Scientific Research  
Bolling Air Force Base  
Washington, DC 20332

Administrative Contracting Officer

Office of Naval Research Laboratory  
(address varies - obtain from Business Office)

Final and Technical Reports Only

Director, Naval Research Laboratory (6 copies)  
Attn: Code 2627  
Washington, DC 20375

E W D

10 - 86

DT / C